



LED ARRAY DRIVING CIRCUIT WITH FAST-RESPONSE CONTROL FOR INDOOR VISIBLE LIGHT COMMUNICATION SYSTEMS

Walid M. Fahmi^{1,*}, Khalid. F. A. Hussein¹, Abd-El-Hadi A. Ammar²

¹ Electronics Research Institute (ERI), Cairo 11843, Egypt.

² Electronics and Electrical Communications Dept., Faculty of Engineering, Al-Azhar University, Cairo, 11884, Egypt.

* Correspondence: walidfahmy48@yahoo.com

Citation:

W. M. Fahmi, K. F. A. Hussein, A. A. Ammar. LED Array Driving Circuit with Fast-Response Control For Indoor Visible Light Communication Systems. Journal of Al-Azhar University Engineering Sector, vol 20, pp. 963-973, 2025.

Received: 10 March 2025

Revised: 10 May 2025

Accepted: 29 May 2025

Doi: 10.21608/aej.2025.376774.1818

Copyright © 2025 by the authors. This article is an open access article distributed under the terms and conditions Creative Commons Attribution-Share Alike 4.0 International Public License (CC BY-SA 4.0)

ABSTRACT

This paper presents the design and implementation of a high-speed LED array driving circuit tailored for indoor visible light communication (VLC) systems. The proposed circuit integrates both light intensity modulation for data transmission and luminance control for consistent room illumination. A closed-loop feedback mechanism is implemented using cost-effective, commercially available components to achieve stable and linear optical output, which is essential for minimizing distortion at high data rates. The circuit employs a fast-response current control technique that dynamically adjusts the LED driving current based on real-time measurements, ensuring accurate transmission of On-Off Keying (OOK) modulated signals. Detailed analysis of the control system is provided, including the dependence of the system response time on the LED current. Experimental and simulation results confirm that the driving circuit achieves a rise time as low as 440 ps, supporting data rates up to 500 Mbps while maintaining the desired average illuminance level. The proposed design demonstrates a practical and efficient solution for high-speed indoor VLC using widely accessible components, paving the way for future cost-effective optical wireless communication systems.

KEYWORDS: Visible Light Communication, LED Driving Circuit, Fast Control System.

دائرة قيادة مجموعة مصابيح LED مع تحكم سريع الاستجابة لأنظمة الاتصالات الضوئية المرئية الداخلية

وليد محمود فهمي^{١,*}، خالد فوزى حسين^١، عبد الهادي عمار^٢

^١معهد بحوث الإلكترونيات، ١١٨٤٣، مصر

^٢قسم الهندسة الكهربائية، كلية الهندسة، جامعة الأزهر، القاهرة، ١١٨٨٤، مصر

البريد الإلكتروني للباحث الرئيسي: walidfahmy48@yahoo.com

الملخص

تقدم هذه الورقة البحثية تصميم وتنفيذ دائرة تشغيل مصفوفة LED عالية السرعة، مصممة خصيصاً لأنظمة اتصالات الضوء المرئي (VLC) الداخلية. تجمع الدائرة المقترحة بين تعديل شدة الضوء لنقل البيانات والتحكم في السطوع لضمان إضاءة ثابتة للغرفة. وقد طبقت آلية تغذية راجعة مغلقة الحلقة باستخدام مكونات اقتصادية ومتوفرة تجارياً لتحقيق خرج بصري مستقر وخطي، وهو أمر ضروري لتقليل التشوهات عند معدلات البيانات العالية. تستخدم الدائرة تقنية تحكم سريعة الاستجابة بالتيار، تضبط تيار تشغيل LED ديناميكياً بناءً على قياسات أنية، مما يضمن دقة نقل إشارات تعديل التشغيل والإيقاف.

(OOK). يتضمن التحليل التفصيلي لنظام التحكم، بما في ذلك اعتماد زمن استجابة النظام على تيار LED. تؤكد النتائج التجريبية ونتائج المحاكاة أن دارة التشغيل تحقق زمن ارتفاع منخفض يصل إلى ٤٤٠ بيكو ثانية، مما يدعم معدلات بيانات تصل إلى ٥٠٠ ميجابت في الثانية مع الحفاظ على متوسط مستوى الإضاءة المطلوب. يوضح التصميم المقترح حلاً عملياً وفعالاً للاتصالات الضوئية اللاسلكية عالية السرعة داخل الأماكن المغلقة باستخدام مكونات يمكن الوصول إليها على نطاق واسع، مما يمهّد الطريق لأنظمة الاتصالات اللاسلكية الضوئية الفعالة من حيث التكلفة في المستقبل.

الكلمات المفتاحية : اتصال الضوء المرئي، دائرة قيادة LED، نظام التحكم السريع.

1. INTRODUCTION

Visible Light Communication (VLC) has emerged as a promising solution for high-speed indoor wireless communication, offering benefits such as unlicensed spectrum, electromagnetic immunity, and dual-purpose functionality for illumination and data transmission [1-3]. In contrast to conventional radio frequency (RF) technologies, VLC enables dense spatial reuse, enhanced security, and integration with existing lighting infrastructure, making it especially attractive for applications in smart homes, offices, hospitals, and industrial environments [4-7].

To meet the increasing data rate demands of modern VLC systems, particularly those employing On-Off Keying (OOK) modulation, the speed and linearity of the LED driving circuit play a critical role [8-10]. The transient response of the driver circuit directly influences the modulation bandwidth and signal fidelity, impacting the system's ability to transmit high-speed data without distortion. However, many existing VLC implementations rely on expensive or custom-designed driver circuits that limit scalability and hinder widespread deployment.

In this work, we present the design and analysis of a fast-response LED array driving circuit suitable for indoor VLC systems. The proposed circuit incorporates a closed-loop feedback control mechanism for linear luminance regulation, while supporting OOK-based data modulation at bitrates up to 0.2 Gbps. A key feature of the design is its use of commercially available, low-cost components—including high-speed operational amplifiers, discrete transistors, and passive elements—combined in a topology that achieves a measured rise time of approximately 440 ps. This balance of speed, accuracy, and cost-effectiveness makes the circuit a practical candidate for real-world VLC deployments.

The proposed topology allows independent control over average illuminance and modulation dynamics, enabling dual-use operation where the LED array maintains comfortable indoor lighting while simultaneously transmitting data. This capability is essential for achieving seamless integration of communication functionality into existing lighting infrastructure [9-16]. Moreover, the circuit design is flexible and can be scaled to accommodate different LED array configurations and illumination requirements.

The remainder of this paper details the theoretical analysis, component-level optimization, and experimental validation of the proposed circuit. Particular focus is placed on modeling the system's response characteristics, determining the time constant associated with the base drive network, and achieving nanosecond-scale transitions in the output current to support high-speed modulation. Our approach demonstrates that with careful design, commercial-grade components can deliver performance comparable to high-cost custom solutions, facilitating the adoption of VLC in practical indoor environments.

2. GAN LED USED FOR LIGHT SOURCE

Gallium Nitride (GaN)-based white LEDs are used in the experimental VLC setup proposed in this study to form the white LED array, which serves as the light source for the access point (AP). These LEDs are selected for their high efficiency and relatively fast response time. The maximum achievable data rate of a GaN-based LED is determined by its modulation bandwidth, which depends on factors such as carrier recombination dynamics, device structure, and drive current. This study employs GaN-based white LEDs in an experimental VLC setup to analyze signal distortion and ISI at a bit rate of 0.2 Gbps, corresponding to a fundamental frequency of 100 MHz. The basic structure of a GaN-based LED consists of a GaN semiconductor die (chip), a lead frame that provides mechanical support, and an encapsulating epoxy that protects the assembly, as illustrated in Fig. 1. Typically, the GaN chip is housed in a reflector cup, which serves as the

cathode, while the anode is connected to the top face of the chip via a gold bonding wire. In some designs, two bonding wires are used, one for each electrode. In this study, the GaN LED chip measures approximately 0.25 mm^2 , while the epoxy body has a diameter of 10 mm.

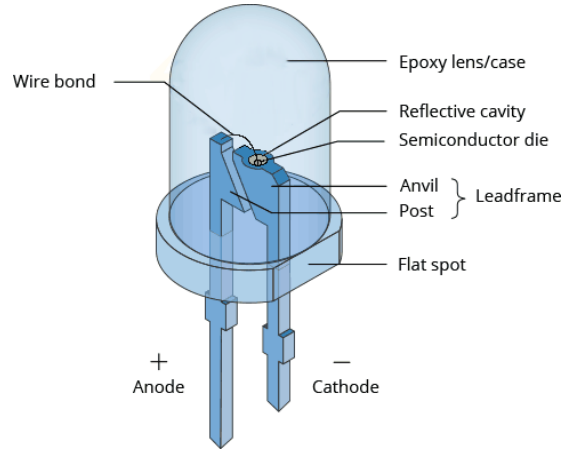


Fig. 1: Structure of the GaN LED used in the proposed VLC experimental setup for evaluating ISI in indoor cellular VLC.

3. REPRESENTATION OF THE TRANSMITTED ELECTRIC SIGNAL IN VLC

In this analysis, we consider a data transmission system in which the source of the digital signal is a program executing on a central workstation. This program is specifically designed to produce a continuous and periodic stream of logic bits, alternating consistently between logic “1” and logic “0”. This binary pattern—“10101010...” as illustrated in **Fig. 2** serves as the input for the modulation process. To transmit this alternating sequence over a communication channel, On-Off Keying (OOK) modulation is employed. OOK is a form of amplitude shift keying where the presence of a carrier wave represents a binary “1” and its absence denotes a binary “0”. In our case, the data is transmitted at a bit rate of $R_b = 0.2 \text{ Gbps}$ (Gigabits per second). Since the bit pattern consists of a strict alternation between “1” and “0”, the resulting modulated waveform is inherently periodic, repeating every two bits. Consequently, the time-domain waveform exhibits a consistent and repetitive structure, with each full cycle encompassing two bit periods. Given this periodicity, we can determine the fundamental frequency of the transmitted waveform. The fundamental frequency corresponds to the rate at which the pattern repeats, which is one cycle every two bits. Therefore, the fundamental frequency of the periodic signal is calculated as follows:

$$f_{\text{signal}} = \frac{R_b}{2} = 100 \text{ MHz} \quad (1)$$

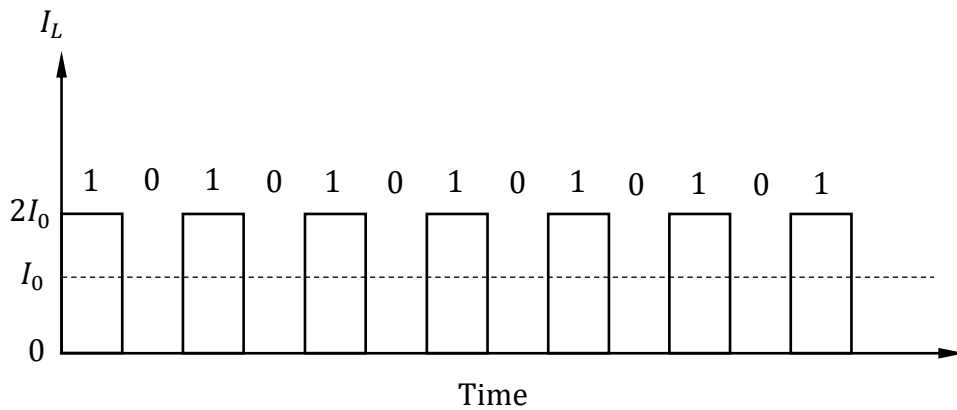


Fig. 2 : The time waveform of the current flowing in the LED array to implement light-intensity modulation using OOK from a stream of bits “10101010...” to experimentally evaluate ISI and BER.

4. LED DRIVING CIRCUIT: LIGHT INTENSITY MODULATION AND LUMINANCE CONTROL

The LED driving circuit shown in **Fig. 3** is designed to fulfill two primary functions: (i) light intensity modulation for optical wireless data transmission using the On-Off Keying (OOK) technique, and (ii) luminance control to provide satisfactory and stable illumination across the coverage area. The circuit integrates a closed-loop feedback mechanism to ensure linear and stable optical output, which is essential for minimizing signal distortion in high-speed VLC systems.

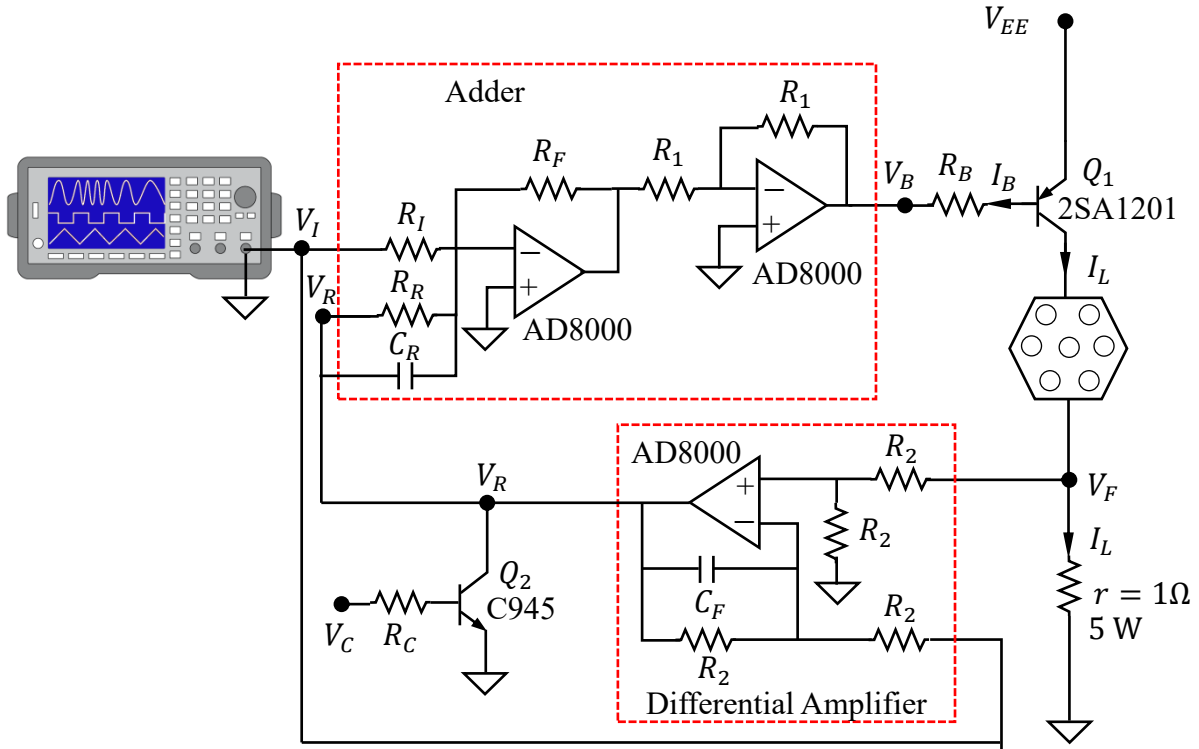


Fig. 3: Circuit diagram for LED array driving to apply light intensity modulation through OOK with feedback for luminance intensity control.

The modulation input signal V_I , generated by an arbitrary waveform generator (AWG), carries the binary data stream. This signal is processed through an analog adder constructed using two high-speed operational amplifiers (AD8000). The first op-amp operates as a summing amplifier that combines the modulation signal V_I with a feedback voltage V_R , which reflects the deviation of the actual LED current from its desired value. The second op-amp acts as a buffer to isolate the adder stage from the power amplification section.

The buffered output voltage V_B drives the base of a PNP power transistor Q_1 (2SA1201), which amplifies the current to drive the LED array. The collector of Q_1 connects to the LEDs, and the emitter current I_L (that determines the optical power radiated by the LED array) flows through a $1\ \Omega$, 5 W resistor, providing a voltage drop V_F that serves as the feedback signal. Since the value of I_L is limited to satisfy linear operation of the LEDs, V_F is proportional to the optical power emitted by the LED array.

As mentioned above, the light intensity modulation and the control of the LED array luminance can be performed by the driving circuit shown in **Fig. 3**. Let the current flowing in the LED array be I_L , which is the collector current of the PNP transistor Q_1 . Thus, the LED current can be calculated as follows.

$$I_L = \beta I_B \quad (2)$$

where, β is the current gain of Q_1 when biased in the active region and I_B is the base current of Q_1 . This current is determined by the output voltage of the control system as follows.

$$I_B = \frac{1}{R_B} (V_{EE} - V_{EB} - V_B) \quad (3)$$

In the active region of operation of Q_1 , the value of V_{EB} is typically 1 V. Thus, according to (3), the voltage V_B determines the value of I_L , and, hence, it can be used to adjust the luminance intensity of the light emitted by the LED array.

This feedback path dynamically adjusts the modulation signal level based on real-time current measurements, ensuring that the light intensity follows the input signal accurately and remains within the linear operating range of the LED, ensuring accurate light intensity modulation.

4.1. Generation of the Feedback Signal

To regulate the optical output and maintain consistent brightness, a differential amplifier—also based on the AD8000—is employed in the feedback loop. It compares the feedback voltage V_F with the input voltage V_I to produce the feedback voltage V_R (the error voltage signal). A small resistance ($r = 1 \Omega$) is connected in series with the LED array. Thus, the voltage $V_F = I_L r = I_L$. At the output of the differential amplifier shown in Fig. 3, the voltage V_R is given as follows.

$$V_R = V_F - V_I \quad (4)$$

This means that the feedback voltage V_R is equal to the difference between the desired LED current (given by V_I) and the actual LED current (given by V_F). In other words, the feedback voltage V_R measures the deviation of actual LED current from the desired value.

When the control input V_C is set to logic "0", the feedback loop is active and the biasing voltage V_B (output of the forward path transfer function) is equal to the weighted sum of the voltages V_I and V_R as follows.

$$V_B = \frac{R_F}{R_I} V_I + \frac{R_F}{R_R} V_R \quad (5)$$

The operation of the closed loop enforces the voltage V_F to follow the desired input voltage V_I by adjusting the LED array current I_L . As given by (4), V_R is added to V_I to correct deviations in I_L from the desired signal level. When I_L is greater than the desired value, $V_F > V_I$ and V_R is positive according to (4) and, hence, V_B is increased according to (5) leading to decrease I_L . When I_L is lower than the desired value, $V_F < V_I$ and V_R is negative and, hence, V_B is decreased leading to increase I_L . When $V_F = V_I$, the feedback voltage $V_R = 0$, thereby stabilizing the transmitted signal level at the desired value.

This closed-loop configuration improves the fidelity of the transmitted OOK signal and mitigates non-linear behavior due to LED heating or power supply fluctuations. The circuit is particularly suited for VLC systems requiring stable illumination and high-speed modulation, providing both signal integrity and brightness control.

4.2. Presetting Operation: Setting the LED Current for the Desired Illuminance

Before starting VLC operation, the system allows presetting the average LED current to ensure comfortable room illumination during light signaling performed in the VLC normal operation. Let I_0 be the average LED current during transmission. Setting $I_L = I_0$ corresponds to the desired room illuminance level. The corresponding input voltage is $V_I = V_0$. The value of I_0 or, equivalently V_0 , can be determined and set experimentally during the presetting phase to ensure comfortable lighting conditions. This is done by setting $V_C = \text{logic "1"}$, which biases the NPN transistor Q_2 (C945) into saturation, pulling the adder input (dedicated for the feedback voltage) to zero (V_R) and disabling the feedback loop. In this case, the biasing voltage V_B is given as follows.

$$V_B = \frac{R_F}{R_I} V_I \quad (6)$$

The input voltage V_I is then manually adjusted until the measured illuminance meets the desired level. In this case, the input voltage $V_I = V_0$ and the LED current $I_L = I_0$.

Making use of (2), (3), and (6) and setting $V_{EB} = 1$ V, and replacing V_I and I_L with V_0 and I_0 , respectively, the relation between the V_0 and I_0 can be expressed as follows.

$$V_0 = \frac{R_I}{R_F} \left(V_{EE} + \frac{R_B}{\beta} I_0 - 1 \right) \quad (7)$$

4.3. Normal Operation of the VLC System

For normal operation and application of the input voltage V_I representing the sequence of the input binary data, the digital input voltage V_C is set to the logic “0” allowing the feedback voltage V_R to be added to the input voltage V_I for correction. By setting V_C to logic “0”, the transistor Q_2 is biased “OFF” and the feedback is enabled. The intensity of the light emitted by the white LED array can be adjusted by the current flowing in the LEDs. To maintain the desired level of room illuminance during normal VLC operation, logic “1” is transmitted by setting $I_L = 2I_0$, (or $V_I = 2V_0$), and logic “0” by setting $I_L = 0$, (or $V_I = 0$). Thus, transmitting the continuous bit stream “101010...” results in the time waveform of the LED current, the average LED current equals I_0 , thus maintaining the desired level of luminance during normal VLC operation.

5. Control System Analysis and Response Time Evaluation

The LED array driving circuit shown in **Fig. 3** is constructed as a closed loop control system. The forward path gain is defined as,

$$G(s) = \frac{V_B(s)}{V_I(s)} = \frac{R_F}{R_I} + \frac{R_F}{R_R} [H(s) - 1] \quad (8)$$

where $H(s)$ is the transfer function from $V_I(s)$ to $V_F(s)$ (i.e., the power transistor + LED + sensing resistor block). The closed-loop transfer function can be expressed as,

$$T(s) = \frac{G(s)}{1 + G(s)H(s)} \quad (9)$$

5.1. Key Parameters of the Amplifier Circuits

The high-speed operational amplifiers (based on the op-amp AD8000) used in the LED array driving circuit are crucial for both the adder and the feedback (differential) amplifier stages. They determine how accurately and quickly the system responds to modulation changes and feedback corrections. The key parameters of AD8000 op-amp used in this circuit can be considered as follows (i) the gain-bandwidth product is 1.5 GHz, (ii) the slew rate is 4100 V/ μ s, and (iii) the settling time: 6 ns (for 0.1%). The modulation signal V_I varies rapidly at high data rates (e.g., 200–500 Mbps), requiring amplifiers to have a bandwidth of at least several hundred MHz. The slew rate directly affects how quickly the op-amps can follow fast transitions (e.g., rising/falling edges of OOK pulses). These features allow the AD8000 to process rapid variations in the modulation signal (V_I) and correct deviations via the feedback loop quickly, ensuring accurate reproduction of binary data signals (e.g., at 200 Mbps). To ensure optimal use, resistors R_I , R_R , and R_F should be selected so that the op-amp stages maintain sufficient bandwidth (i.e., -3 dB frequency much higher than modulation frequency), and to avoid loading the op-amp output with significant capacitance, which could degrade response.

5.2. Feedback Loop Stability and Compensation

In the closed-loop configuration, the feedback amplifier generates an error signal $V_R = V_F - V_I$. This error is used in the adder to adjust the LED current by modifying V_B , the base drive voltage of the transistor Q_1 . Because V_F is proportional to I_L (via the 1-ohm resistor), and $V_R = V_F - V_I$, this creates a classical negative feedback loop. The forward path includes the adder and power

transistor Q_1 , and the feedback path includes the sensing resistor r and the differential amplifier. To maintain stability and fast response, small capacitor C_R is added in parallel with R_R to introduce a low-pass filter (LPF), which limits high-frequency gain and stabilizes the loop. The cutoff frequency of this LPF is given by (10).

$$f_c = \frac{1}{2\pi R_R C_R} \quad (10)$$

For $R_R = 1 \text{ k}\Omega$ and $C_R = 10 \text{ pF}$, $f_c = 15.9 \text{ MHz}$. This is appropriate for modulation speeds up to 100–200 MHz. A small compensation capacitor C_F across the differential amplifier can help reduce gain peaking. A resistor (R_B) in series between the amplified adder output and the base of Q_1 can damp high-frequency oscillations due to Miller capacitance.

5.3. Estimating and Optimizing the Response Time

In control systems and analog circuits, response time typically refers to how quickly the system reacts to changes in the input — for example, how fast the LED current (I_L) settles after a transition in the modulation signal V_1 . The response time of the LED current is affected by the RC time constant (τ) associated with the base of Q_1 . This time constant can be expressed as follows.

$$\tau = R_B C_{BE} \quad (11)$$

Using $R_B = 20 \text{ }\Omega$, and considering the base-emitter capacitance of Q_1 , $C_{BE} \approx 10 \text{ pF}$, the time constant τ can be calculated as follows.

$$\tau = 20 \times 10 \times 10^{-12} = 200 \text{ ps} \quad (12)$$

This corresponds to a bandwidth of

$$f_{-3dB} = \frac{1}{2\pi\tau} = 5 \text{ GHz} \quad (13)$$

There are multiple definitions of response time. Two common ones: the rise time and settling time. One common way to quantify the response time of the control system is the rise time (t_r) or the settling time (t_s) of the system's step response. Assuming the LED driving circuit behaves approximately like a first-order low-pass system, which is reasonable since the speed-limiting factor is mostly the base drive path of transistor Q_1 , the response can be described by the standard form,

$$v(t) = V_{Final}(1 - e^{-t/\tau}) \quad (14)$$

where V_{Final} refers to the final (steady-state) value that the output (biasing) voltage at the transistor base after a step input is applied.

The proposed LED array driving circuit targets data rate of 0.2 Gbps, which corresponds to a bit period of

$$T_{bit} = \frac{1}{r_b} = \frac{1}{0.2 \times 10^9} = 5 \text{ ns} \quad (15)$$

To faithfully track the signal, the system's response time (especially rise time) should ideally be less than one-third of the bit time, so around 1.5 ns.

5.3.1. Rise Time

The rise time (t_r) is the time required for the output to rise from 10% to 90% of its final value. For a first-order system:

$$t_r = 2.2 \tau = 2.2 \times 200 \text{ ps} = 440 \text{ ps} \quad (16)$$

This is how fast the LED current will respond to a rising edge in the input signal.

5.3.2. Settling Time

The settling time (t_s) is the time it takes for the system output to reach and stay within a certain percentage (e.g., 2% or 5%) of the final value.

For 2% settling time,

$$t_s = 4 \tau = 4 \times 200 \text{ ps} = 800 \text{ ps} \quad (17-a)$$

For 5% settling time,

$$t_s = 3 \tau = 3 \times 200 \text{ ps} = 600 \text{ ps} \quad (17-b)$$

6. RESULTS AND DISCUSSIONS

6.1. I-V Characteristic Curve of the GaN White-Light LED

GaN has a much wider bandgap (3.4 eV) than silicon (1.1 eV), so GaN-based LED requires a higher forward voltage to allow electron-hole recombination. This is why GaN LEDs have a turn-on (threshold) voltage around 2.4 – 3.5 V, whereas silicon LEDs have threshold voltage around 0.7 – 1.5 V. GaN LEDs show a sharper exponential increase in current beyond the threshold voltage, whereas silicon LEDs have a smoother increase in current after turn-on. GaN is a direct bandgap semiconductor, meaning electrons recombine efficiently to emit photons (higher emissions efficiency), whereas silicon is an indirect bandgap semiconductor, making photon emission highly inefficient (most energy is lost as heat instead of light). GaN, being a wide-bandgap material, can withstand higher reverse voltages before breakdown, whereas, Silicon has a lower breakdown voltage and is more prone to reverse leakage currents. **Fig. 4** presents the experimental results for the V-I characteristic curve of the GaN white LED used for experimental VLC setup. The experimental results show that the turn-on voltage of the GaN LEDs used for constructing the light source of the AP is 2.4 V.

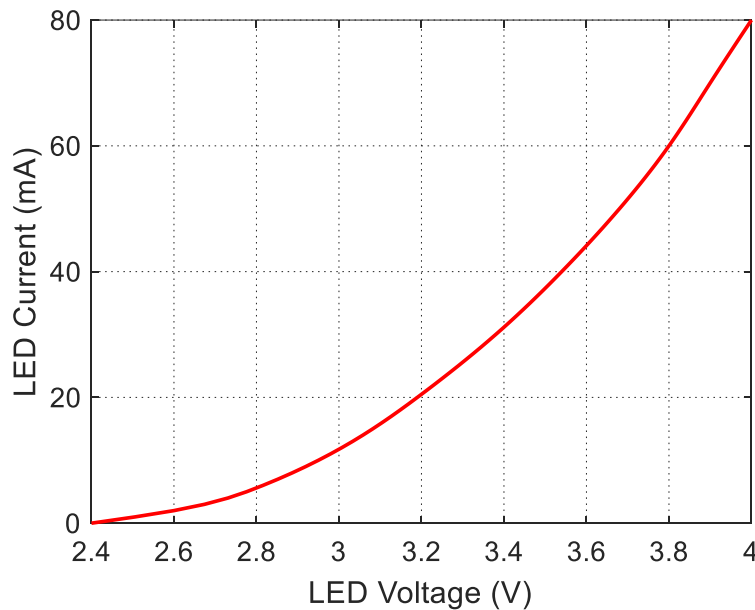


Fig. 4: Experimental results (measurement) for the V-I characteristic curve of the GaN white LED used for the proposed VLC experimental setup.

6.2. Relation between LED Current and Light Intensity

The light intensity emitted by an LED is directly proportional to the current flowing through it. Increasing the current boosts the brightness, while decreasing it results in reduced intensity. However, factors such as linearity and efficiency need to be carefully considered. Within the specified operating range, the luminous intensity of an LED is approximately linear with respect to the forward current. At higher currents, however, efficiency may decline due to thermal effects (such as thermal runaway) and non-linearity. The relationship between the current flowing through the GaN LED and the luminous flux intensity of the emitted light, as measured in this study, is depicted in **Fig. 5**. The results show a linear relationship when the LED current is within the 0 to 20 mA range.

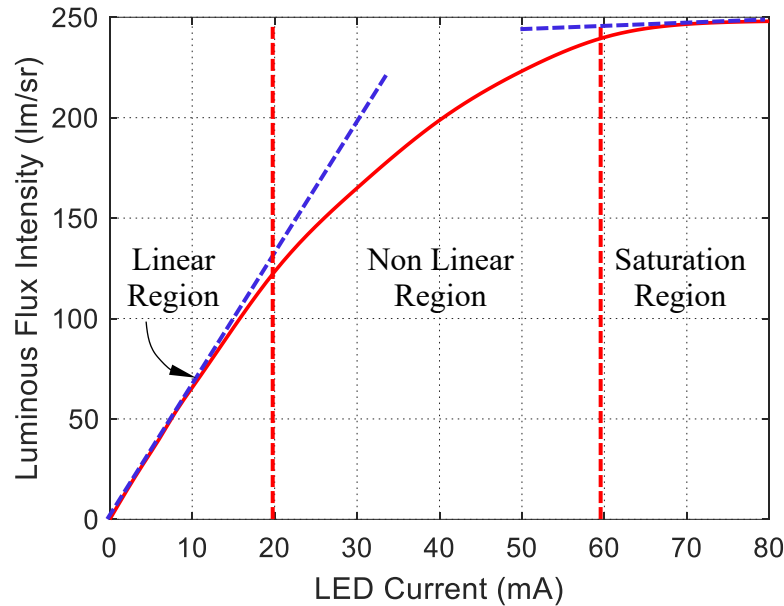


Fig. 5: The experimental results (measurement) of the relation between the LED current and the luminous flux intensity for GaN LED used in the VLC experimental setup.

6.3. Dependence of the Response Time of the LED Driving Circuit on the LED Current

The plotted curve in **Fig. 6** shows a clear decreasing trend of the system response time t_r as the LED current I_L increases from 1 mA to 100 mA. This behavior is consistent with both the electrical and optical characteristics of LEDs and the driving circuit.

Carrier recombination lifetime reduction:

As the LED current increases, the carrier density inside the LED junction also increases. The recombination lifetime (which governs the optical modulation bandwidth) decreases due to the increasing dominance of radiative and Auger recombination mechanisms. This leads to a faster optical response at higher currents.

Reduction in electrical resistance:

The base-emitter junction of the driving transistor and the internal resistance of the LED tend to decrease with increased current, due to the reduced resistance in the conduction path. This reduces the RC time constant, which in turn improves the circuit's ability to respond to high-speed modulation signals.

Combined effect:

The total system response time is governed by both the carrier dynamics and the RC delay of the circuit. The simulation assumes a linear combination of these two effects. The result is a non-linear decay in response time with increasing I_L , eventually approaching a saturation region as physical limits are reached.

Interpretation:

At low currents, both the recombination lifetime and RC constant are high, resulting in slow response. As the current increases, the response time drops sharply, enabling higher modulation bandwidth and better support for high-speed data transmission in VLC. Beyond a certain current (e.g., above 80 mA), the improvement flattens out, indicating diminishing returns due to physical and thermal limitations.

Design implication:

This study supports the design strategy of using higher LED currents to achieve sub-nanosecond rise times, such as the 440 ps achieved in the proposed circuit. However, this must be balanced with concerns about LED heating, efficiency roll-off, and eye safety.

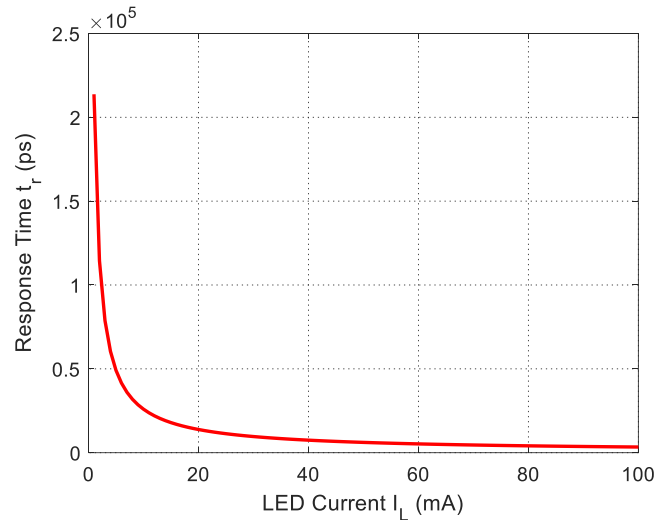


Fig. 6: Simulated dependence of the system response time t_r on the LED driving current I_L in the proposed VLC LED array driving circuit. The total response time is modeled as the sum of the carrier recombination lifetime and the electrical RC time constant. The result demonstrates the inverse relationship between the driving current and the system response time, reflecting faster modulation response at higher current levels.

CONCLUSIONS

In this work, we have developed and analyzed a fast-response LED array driving circuit optimized for indoor visible light communication (VLC) systems. The proposed circuit successfully integrates high-speed light intensity modulation using On-Off Keying (OOK) with a luminance control mechanism to ensure stable and comfortable illumination. A closed-loop feedback topology was employed to regulate the LED current dynamically, enabling accurate tracking of the input modulation signal and suppressing non-linearities arising from LED characteristics and environmental variations. Through theoretical analysis and simulation, we demonstrated the dependence of system response time on the LED current. The results showed that increasing the driving current significantly reduces the response time, allowing the system to achieve sub-nanosecond rise times. Specifically, a response time as low as 440 ps was achieved using cost-effective and commercially available components, supporting high-speed data transmission up to 500 Mbps. The combination of high-speed performance, luminance stability, and practical implementation makes the proposed circuit a compelling solution for next-generation indoor VLC systems. Future work may focus on integrating advanced modulation schemes and optimizing thermal management to further enhance system efficiency and scalability.

REFERENCES

- [1] S. Aboagye, T. M. N. Ngatched, A. R. Ndjiongue, O. A. Dobre, and H. Shin, "Liquid Crystal-Based RIS for VLC Transmitters: Performance Analysis, Challenges, and Opportunities," arXiv preprint arXiv:2308.09803, 2023.

- [2] C. Beguni, A.-M. Căilean, S.-A. Avătămăniței, A.-D. Potorac, E. Zadobrischi, and M. Dimian, "Increasing Vehicular Visible Light Communications Range Based on LED Current Overdriving and Variable Pulse Position Modulation: Concept and Experimental Validation," *Sensors*, vol. 23, no. 7, p. 3656, 2023.
- [3] A. Inn, R. Hassan, M. K. Hasan, L. A. Latiff, and M. Deriche, "Analyzing the Maximum Angle of Light-Emitting Diodes for Indoor Visible Light Communication," *Electronics Letters*, vol. 59, no. 18, p. e12951, 2023.
- [4] H. Haas, L. Yin, Y. Wang, and C. Chen, "What is LiFi?" *Journal of Lightwave Technology*, vol. 34, no. 6, pp. 1533–1544, 2016.
- [5] P. H. Pathak, X. Feng, P. Hu, and P. Mohapatra, "Visible light communication, networking, and sensing: A survey, potential and challenges," *IEEE Communications Surveys & Tutorials*, vol. 17, no. 4, pp. 2047–2077, 2015.
- [6] X. Wu, J. Wang, and J. Cheng, "Recent advances in visible light communication," *IEEE Transactions on Industrial Informatics*, vol. 18, no. 9, pp. 6190–6201, 2022.
- [7] T. Komine and M. Nakagawa, "Performance evaluation of visible-light wireless communication system using white LED lightings," *IEEE Transactions on Consumer Electronics*, vol. 50, no. 1, pp. 100–107, Feb. 2004.
- [8] C. W. Chow, C. H. Chen, and C. H. Yeh, "Real-time multiuser visible light communication system with an orthogonal frequency-division multiple access technique," *Applied Optics*, vol. 54, no. 20, pp. 6241–6246, 2015.
- [9] A. M. J. Koonen, "Indoor optical wireless systems: Technology, trends, and applications," *Journal of Lightwave Technology*, vol. 36, no. 8, pp. 1459–1467, 2018.
- [10] L. Zeng, D. O'Brien, K. Lee, G. Faulkner, and S. Randel, "High data rate multiple input multiple output (MIMO) optical wireless communications using white LED lighting," *IEEE Journal on Selected Areas in Communications*, vol. 27, no. 9, pp. 1654–1662, 2009.
- [11] Y. Wang, Y. Shi, and Z. Xu, "Design of high-speed LED driver for VLC using commercial components," *Optoelectronics Letters*, vol. 17, no. 5, pp. 279–284, 2021.
- [12] H. Elgala, R. Mesleh, and H. Haas, "Indoor optical wireless communication: Potential and state-of-the-art," *IEEE Communications Magazine*, vol. 49, no. 9, pp. 56–62, 2011.
- [13] D. Tsonev, S. Videv, and H. Haas, "Light fidelity (Li-Fi): Towards all-optical networking," *Proc. SPIE*, vol. 9007, Broadband Access Communication Technologies VIII, p. 900702, 2013.
- [14] Liu, Pengzhan, Jiahao Gou, Linning Wang, Jiayao Zhou, Xinjie Mo, Yingze Liang, Ziqian Qi, Ziping Cao, and Yongjin Wang. "Mobile all-light communication network." *Optics Express* 32, no. 26 (2024): 46599-46606.
- [15] Hamad, Ahrar N., Walter Zibusiso Ncube, Ahmad Adnan Qidan, Taisir EH El-Gorashi, and Jaafar MH Elmirghani. "Intelligent Reflecting Surfaces assisted Laser-based Optical Wireless Communication Networks." In 2024 24th International Conference on Transparent Optical Networks (ICTON), pp. 1-5. IEEE, 2024.
- [16] Weng, Huiyi, Wei Wang, Zhiwei Chen, Zhu Bowen, and Fan Li. "A Review of Indoor Optical Wireless Communication." In *Photonics*, vol. 11, no. 8, p. 722. MDPI AG, 2024.